

UC Office of the President

UCOP Previously Published Works

Title

X-ray Absorption and Emission Spectroscopy Study of the Effect of Doping on the Low Energy Electronic Structure of PrFeAsO_{1- δ}

Permalink

<https://escholarship.org/uc/item/7w69n8sq>

Journal

Journal of the Physical Society of Japan, 79(7)

Author

Freelon, Byron

Publication Date

2010-07-12

Peer reviewed

X-ray Absorption and Emission Spectroscopy Study of the Effect of Doping on the Low Energy Electronic Structure of PrFeAsO_{1-δ}

Byron FREELON,¹ Yi-sheng LIU,² Costel. R. ROTUNDU,³ Stephen. D. WILSON,³ Jinghua GUO,⁴ Jeng-Lung CHEN,^{2,4} Wanli. YANG,⁴ Chunli. CHANG,² Per. Anders. GLANS,⁴ Parasharam. SHIRAGE,⁵ Akira. IYO,⁵ and Robert. J. BIRGENEAU^{1,3}

¹*Department of Physics, University of California, Berkeley, CA 94720*

²*Department of Physics, Tamkang University, Tamsui, Taiwan 250*

³*Materials Science Division, Lawrence Berkeley National Laboratory, Berkeley, CA 94720*

⁴*Advanced Light Source, Lawrence Berkeley National Laboratory, Berkeley, CA 94720*

⁵*National Institute of Advanced Industrial Science and Technology, Tsukuba, Ibaraki 305-8568, Japan*

We report electronic density of states measurements of oxygen vacated PrFeAsO using soft X-ray absorption and emission spectroscopy. The electronic density of states is observed to undergo doping dependent shifts. Oxygen X-ray absorption and emission show long-range intermixing of oxygen p states. Mean field theory and local density approximations give a good description of the measured oxygen and iron spectra. The near Fermi-level iron spectral weight shows a systematic doping dependence. Concomitant changes in the unoccupied iron-arsenic hybridized spectral features reveal that Fe-As bonding is involved in the process of electron addition near the Fermi-level. By combining X-ray emission and absorption spectra, we observe an increase in the Fe density of states at the Fermi-level as the doping decreases. This doping dependent electronic behavior indicates the possibility of a magnetic instability in the undoped compound. Our data overall imply that PrFeAsO_{1-δ} has weak to intermediate electron correlations.

KEYWORDS: electron correlations, electronic density of states, high-temperature superconductors, iron arsenide compounds, lanthanide compounds, x-ray emission spectra, x-ray absorption spectra, superconducting transitions, valence bands

1. Introduction

An intense flurry of research has been performed on the recently discovered Fe-based rare-earth (*RE*)-pnictide high-temperature superconductors.¹⁾ These compounds form a distinct, novel class of superconducting materials in which *RE*-substitution (*RE* = La, Ce, Pr, Nd, Sm, Gd) in $REFeAsO_{1-x}F_x$ or $REFeAsO_{1-\delta}$ has been found to yield superconducting transition temperatures (T_c) as high as 55K.²⁾ In addition, the related bilayer materials AFe_2As_2 (A = Ba, Sr, Eu and Ca) materials have been found³⁾ to become superconducting upon sufficient K or Na-doping or replacement of the Fe atom by Co or Ni. At this early stage of study, the nature and mechanism of the iron-arsenide superconductivity as well as the basic electronic structure of these materials is still being explored. Current theoretical reports suggest that the parent phase is either a non-magnetic metal or an antiferromagnetic (AF) semi-metal⁴⁾ while experiments confirm the latter. The AF behavior has been shown to diminish progressively as these materials are driven toward superconductivity by doping. The extent to which the FeAs materials are in the vicinity of a Mott insulating phase⁵⁾ is controversial as shown by differences in experimental and theoretical conclusions concerning the degree of electronic correlations.⁶⁾ In addition to the electronic structure, the basic magnetic nature of the parent phase is also debated, although neutron scattering shows convincingly an AF phase below temperatures typically of the order of 140 K. Given the present controversies it is important to study, experimentally, the electronic behavior to compare with that of the cuprates and to reconcile the electronic properties with magnetic information.

FeAs superconductivity can be achieved in the $REFeAsO$ materials by chemical modification of the intermediate *RE*-layers which, in turn, can lead to electron doping of the FeAs planes. Electron-doped, as opposed to hole-doped, FeAs superconductors can be created in at least three ways: Fluorine-substitution for oxygen, oxygen deficiency, and the substitution of Th^{4+} for RE^{3+} . All of these steps occur in the charge reservoir *RE*-O layer by

substitution and induce electron carriers. The electron doping, in turn, induces charge transfer to the Fe-As layer that results in superconductivity.

The effect of electron-doping on the electronic structure has been studied theoretically and experimentally but, so far, the conclusions are indefinite. To-date, local density approximation (LDA), dynamical mean field theory (DMFT), and spin-dependent LDA (LDSA) calculations have given differing results on the question of whether or not the FeAs family of superconductors are strongly correlated. Haule *et al.*,⁷⁾ using DMFT, concluded that the materials are strongly correlated. In contrast, Kurmaev *et al.*,⁸⁾ and Yang *et al.*,⁹⁾ based on Fe 3d electronic structure measurements by x-ray absorption and emission spectroscopy, suggested the absence of strong electronic correlations. Angle-resolved¹⁰⁾ and -integrated¹¹⁾ photoemission spectroscopy results from the first reported iron-based superconductor, LaFeOP, as well as LaFeAsO_{1-x}F_x, support proposed itinerant magnetism ground state models of these materials. Such a claim is at odds with the strongly correlated electron picture that emphasizes an antiferromagnetic (AF) ground state Mott physics interpretation.

In this paper, we report measurements of the low-energy, near the Fermi-level E_F , electronic structure in the set of materials PrFeAsO_{1- δ} with $\delta = 0.15, 0.30$ and 0.35 . Soft x-ray absorption and emission spectroscopy (XAS and XES) are used to extract element specific density of states (DOS) spectra that can be directly compared to theoretical calculations of the electronic structure of the PrFeAsO materials. The obtained spectra show a remarkable consistency among the spectral features across samples of various doping. This gives the authors confidence that the measured features are real and not, for example, due to impurities which would vary from sample to sample. The evolution of the low-energy oxygen partial density (DOS) as a function of oxygen vacancy is presented and discussed in the context of hybridization within the RE-O and FeAs layers. Measurements of the Fermi-level crossing Fe 3d states reveal a single, narrow dominant peak having an As hybridization shoulder in

agreement with other experimental⁸⁾ and theoretical¹²⁾ results. The Fe conduction band onset is shown to undergo a shift to higher energy as a function of electron doping (oxygen vacancy). An evaluation of Fe XES data gives guidance concerning a reasonable estimate of the Fe 3*d* bandwidth W . Finally, an increase in the Fe electronic density of states at the Fermi-level is demonstrated for less doped samples. This electronic trend indicates an approach toward a magnetic instability in the parent phase of PrFeAsO_{1- δ} .

2. Experimental Procedure

Polycrystalline PrFeAsO_{1- δ} samples were synthesized at high pressure and high temperature using a cubic-anvil high-pressure apparatus.¹³⁻¹⁵⁾ The nominal oxygen deficiencies at the start of the synthesis were $\delta = 0.15, 0.30,$ and 0.35 in PrFeAsO_{1- δ} and we use these δ values to label the data taken on these samples. Neutron scattering analysis¹⁶⁾ of NdFeAsO_{1- δ} showed that the oxygen deficiencies of the synthesized samples tended to be smaller than those of the starting materials which was likely due to the oxidation of the materials during the synthesis process. The same could obtain here as well. The crystal structure of PrFeAsO_{1- δ} is shown in Fig. 1. REFeAsO are quaternary equiatomic compounds that have a rather simple structure of alternating FeAs and RE-O layers with eight atoms in a tetragonal unit cell of space group P4/*nmm* at 300K. The lattice parameters (T_c) of the PrFeAsO_{1- δ} samples are $\hat{a} = 3.9866 \text{ \AA}, \hat{c} = 8.6046 \text{ \AA}; \hat{a} = 3.9770 \text{ \AA}, \hat{c} = 8.5869 \text{ \AA};$ and $\hat{a} = 3.9627 \text{ \AA}, \hat{c} = 8.5721 \text{ \AA}$ for $\delta = 0.15, 0.30,$ and $0.35,$ respectively. The \hat{a} -parameter systematically decreases upon increasing the nominal δ , which means that the oxygen deficiencies of the samples systematically increased though, as stated above, there is some ambiguity in the absolute value of the oxygen deficiency parameter δ . The T_c s of the PrFeAsO_{1- δ} samples $\delta = 0.15, 0.30,$ and 0.35 were measured to be 3 K, 43 K and 48 K, respectively, using a SQUID magnetometer under a magnetic field of 5 Oe after zero-field cooling from sufficiently far above T_c .

X-ray absorption and emission measurements were performed at the Advanced Light Source of the Lawrence Berkeley National Laboratory. XES reflect the occupied partial density of states (DOS) of the valence band while XAS yields the unoccupied partial DOS associated with the conduction band. We employed O $1s$ XAS and O $K\alpha$ -edge XES to investigate the electronic structure of the oxygen-associated bands. O $1s$ XAS entails the $1s \rightarrow 2p$ transition and O $K\alpha$ XES records the intensity resulting from the O $2p \rightarrow 1s$ transition. Transition metal (TM) edge x-ray spectroscopy is highly sensitive to the chemical environment of the TM atoms; therefore, we employed Fe $2p$ XAS and Fe $L_{2,3}$ -edge XES. In an Fe $L_{2,3}$ -edge XA process Fe $2p$ electrons are excited into empty Fe $3d$ states. Fe $L_{2,3}$ XES profiles were obtained by collecting x-ray emission resulting from the $3d \rightarrow 2p$ transition. The oxygen-reduced samples were filed immediately before being placed in the ultra-high vacuum synchrotron end-station. All measurements were performed at room-temperature. At Beamlines 7.0.1 and 8.0.1, the undulators and monochromators produced intense x-ray beams with spot-sizes on the order of 100 microns and energy resolutions of 0.2 eV (0.2 eV) and 0.5 eV (0.6 eV) for oxygen(iron) x-ray absorption and emission, respectively. X-ray absorption spectra were measured in the total fluorescence yield (TFY) mode with a resolving power of $E/\Delta E = 5000$. All spectra were measured with the radiation incident at 20° with respect to the sample surface. Soft x-ray emission spectra were recorded using a grazing-incidence spectrometer with a two-dimensional multi-channel plate detector and a resolution of 0.35 eV. The spectrometer was mounted inside an ultra-high vacuum experimental chamber within the horizontal plane and positioned 90° relative to the incoming photon beam.

3. Results and Discussion

3.1 Oxygen K -edge x-ray absorption emission spectra

Figure 2 shows the total fluorescence yield (TFY) mode of O $1s$ XAS from $\text{PrFeAsO}_{1-\delta}$ ($\delta = 0.15, 0.30, 0.35$). Fluorescence yield signals originate from within the sample

bulk (of order 10^3 \AA) and provide a good representation of the electronic structure without significant contributions from surface contamination and surface states. The O XAS profiles, normalized by setting the maximum peak of each spectrum equal to unity, are plotted in a collapsed fashion showing the main absorption lines **A**, **B**, and **C**. The O 1s XAS data are consistent with numerous LDA band structure calculations.¹⁷⁾ The consensus of theoretical predictions yields the following spectral features: a weak feature at 1 eV, together with more prominent O spectral band features at about 3 eV and 6 eV above E_F . The pre-peak labeled **A** is primarily due to the hybridization of Fe 3d, arsenic and oxygen states according to LDA^{7,12,18-20)} calculations. The main absorption edge **B** is due to the hybridization of Pr 5d states and oxygen. A band, **C**, of features at 537 eV forms due to strong hybridization bonds of oxygen with Pr states. Oxygen LDA band structure calculations show the presence of O 2p DOS in the range 1 to 2 eV above the Fermi-level where the bonding of Fe 3d [*c.f.* Fig. 2(a) of Ref. 18] and As 4p is the strongest. In addition, LDA predicts the spectral weight of the oxygen 2p DOS to be significantly less than that of the Fe or As DOS at low lying energies. The presence of very weak oxygen states near the Fermi-level is not surprising given that the O ions are separated from the FeAs layer. The small O DOS that exists at low energies may be explained in the following way: O 2p orbitals can hybridize with the Pr through Pr 5d states. Pr 5d states, in turn, hybridize with the empty As 5s and relatively long-range As 4p orbitals. Fe 3d electrons form covalent sp^3 bonds with As 4p states in the superconducting layer. This complicated hybridization scheme, based on long-range oxygen intermixing, is consistent with band theory. In Ref [18] Sawatzky *et al.* stressed that the As 4p-Fe interaction is weaker than the planar hybridization found in the cuprates. Reported band structure calculations indicate that the O 2p hybridization in RE-FeAsO materials is even weaker than the Fe-As bonding, but nevertheless, it is clearly present in our experimental and theoretical results just above and below E_F . The long-range intermixing of the oxygen may play a role in the FeAs layer doping. While a doping mechanism based on weak oxygen intermixing might be

plausible, one clearly must also include the electrostatic influence of the doped *RE* layers on the metallic FeAs layers.

The oxygen 1s absorption spectra of $\text{PrFeAsO}_{1-\delta}$ are similar to that of $\text{REFeAsO}_{1-x}\text{F}_x$.²¹⁾ The overall O 1s XAS spectra do not shift significantly with doping δ . We do not observe an onset shift that might reflect a change in the chemical potential. Kroll *et al.*²¹⁾ reported a trend in F-doped LaFeAsO such that onset of the O 1s XAS pre-peak undergoes small shifts toward higher energies with increased electron doping. The O 1s XAS onset shift was interpreted as being due to the change in O Madelung potential and the change in the chemical potential due to electron doping. The positions of the higher energy $\text{PrFeAsO}_{1-\delta}$ ($\delta = 0.15, 0.30$ and 0.35) absorption features **B** and **C** do not vary with doping. This agrees with results from $\text{LaFeAsO}_{1-x}\text{F}_x$ where the higher energy peaks **B** and **C** were stationary with doping and the pre-peak **A** was observed to change position only by 100 meV as x was varied from $x = 0.0$ to 0.1 .²¹⁾ The inset of Fig. 2 contains XAS plotted in a vertical stack showing the stationary behavior of the spectral features over the measured doping range.

In Fig. 3 the XA and XE spectra are plotted to show the occupied and unoccupied oxygen partial density of states (PDOS). The O $K\alpha$ XES contains four major peaks **I-IV**. **I** and **II** are due primarily to Pr, Fe and O hybridization. These features match those in the oxygen spectral weight (DOS) suggested by LSDA+*U* for PrFeAsO .¹⁹⁾ A clear, dual peak structure occurs in the energy range 4.0 to 5.0 eV below E_F . Several FeAs LDA studies predict this structure, we attribute these peaks to be due do to an oxygen band splitting induced by the Pr crystal field.²²⁾ **III** and **IV** are thought to originate from the oxygen hybridization with Fe-*d* and As-4*p* states.⁷⁾ LDA calculations by Sawatzky *et al.*¹⁸⁾ support this spectral assignment [*c.f.* Fig. 2(a) of Ref. 18] by showing As DOS as the strongest spectral contribution located $\sim 2 - 3$ eV below E_F . Arsenic 4*p* orbitals, possessing a longer range than O 2*p* orbitals, interact primarily with Fe states; therefore, As 4*p* orbitals, while bonding to Fe, simultaneously interact with the *RE*-layer, and thereby, may participate in the transfer of charge carriers to the

superconducting layer. This notion is substantiated by two observations i) LDA results show that the As DOS dominates the oxygen spectral weight near the Fermi-level and ii) DMFT, LDA and LSDA+ U calculations suggest that the As contributions are distributed over a broad energy range. Peaks **III** and **IV** both appear to be due to Fe, As, and oxygen hybridization, but in this energy region, according to theoretical calculations, As dominates the near- E_F O spectral weight. This fact may pose challenges in extracting doping dependent trends from O valence band spectra.

3.2 Fe L -edge x-ray absorption and emission spectra

The Fe $L_{2,3}$ x-ray absorption spectrum for PrFeAsO $_{1-\delta}$ ($\delta = 0.15$) is shown in Fig. 4(a). The XA process yields a direct measurement of the unoccupied (hole) states of the Fe $3d$ band. Incident photons were tuned to $L_{2,3}$ -edge energies in order to initiate one-electron processes that excite Fe $2p$ electrons ($2p^63d^6$) into empty Fe $3d$ states ($2p^53d^7$). These transitions produce two major Fe $L_{2,3}$ absorption features at 707.6 eV (Fe $2p_{3/2} \rightarrow$ Fe $3d$) and 720 eV (Fe $2p_{1/2} \rightarrow$ Fe $3d$) that are separated by 12.4 eV due to spin-orbit (S.O.) splitting of the Fe $2p$ states into $2p_{1/2}$ and $2p_{3/2}$. The Fe XA spectral profile, Fig. 4(a)), of PrFeAsO $_{0.85}$ closely matches that of pure Fe-metal.⁹⁾ The shoulder appearing at the high energy tail of the Fe L_3 peak is thought to be due to covalent sp^3 bonds between Fe $3d$ and As $4p$ states.²³⁾ Fe XAS is a very sensitive tool for determining the chemical environment, electronic structure and valence of Fe ions in compounds.^{24,25)} The single-peak structure of the Fe L_3 line in addition to the S. O. splitting of 12.4 eV indicates that the Fe ion of PrFeAsO $_{1-\delta}$ is in a 2+ valence (high spin) state.^{9,26)} Fig. 4(b) displays non-resonant Fe L -edge XE spectra obtained with 740 eV incident photons. The L -edge XE profile of transition metals is composed of two major peaks due to the $3d \rightarrow 2p_{3/2}$ and $3d \rightarrow 2p_{1/2}$ de-excitation transitions. These XES peaks occur at 705 eV (L_3) and ~ 717 eV (L_2) and are separated in energy by the S.O. splitting of the Fe $2p_{j=1/2,3/2}$ states.

The XA spectrum in Fig. 4(a) was reduced from raw data, in Fig. 5(a), taken from the samples $\text{PrFeAsO}_{1-\delta}$ ($\delta = 0.15, 0.30$ and 0.35). Each raw $\text{PrFeAsO}_{1-\delta}$ spectrum consists of the Fe L_3 mainline and an extraneous shoulder on the high-energy tail. The additional spectral feature originates from the crystal field splitting of a small, unreacted portion of one of the starting materials¹⁵⁾ Fe_2O_3 . Of the two major Fe_2O_3 XAS peaks **A*** and **B***, only **B*** appears prominently in the $\text{PrFeAsO}_{1-\delta}$ data. The relative intensity of **A*** and **B*** is well-known for Fe_2O_3 but it is not manifested in the L_3 band of the raw $\text{PrFeAsO}_{1-\delta}$ spectra indicating that Fe_2O_3 has a non-dominant concentration.

The experimental spectra of Fig. 5(a) were fitted to determine the Fe_2O_3 spectral contribution to the $\text{PrFeAsO}_{1-\delta}$ XA profile. A superposition of Gaussian functions, labeled **1** – **4**, was used in a non-linear least squares fit (gray line in Figure 5(b)) to estimate the contribution of four major characteristics (see vertical hash marks) of the raw $\text{PrFeAsO}_{1-\delta}$ spectra. A fit of pure Fe_2O_3 determined the relative magnitudes and widths of the spectral components of the unreacted material. The Fe_2O_3 peaks (see Figure 5(c)) were scaled to the extraneous component, **2**, of the raw $\text{PrFeAsO}_{1-\delta}$ Fe XAS data. This step ensured that the appropriate magnitude of the Fe_2O_3 spectral contribution was attributed to the raw XAS $\text{PrFeAsO}_{1-\delta}$ profiles. The outlined fitting program assumed²⁷⁾ the profile of raw $\text{PrFeAsO}_{1-\delta}$ to be a linear superposition of Fe_2O_3 and the actual $\text{PrFeAsO}_{1-\delta}$ spectral intensity. Thus, Fe_2O_3 was isolated from the raw data to obtain the resulting $\text{PrFeAsO}_{0.70}$ spectral line shape in Fig. 5(d). Similar spectra obtained for $\text{PrFeAsO}_{1-\delta}$ ($\delta = 0.15$ and 0.35) were found to be in excellent agreement with XAS reported^{8,9,21,23,28)} for other iron-arsenide materials. For consistency, this analysis approach was applied to the oxygen XA spectra. We investigated the presence of Fe_2O_3 in the raw $\text{PrFeAsO}_{1-\delta}$ oxygen XAS data. Fe_2O_3 has two crystal-field split pre-peaks (at 530 eV) below the O 1s edge.^{29,30)} An Fe_2O_3 signature is absent from the O 1s XAS pre-peak region of the raw $\text{PrFeAsO}_{1-\delta}$ spectra (Figure 2). The close similarity of the raw $\text{PrFeAsO}_{1-\delta}$ O 1s pre-peaks in all of the samples rules out the presence of random oxygenation

and provides direct evidence that any extraneous oxidation due to Fe_2O_3 is negligibly small³¹⁾ in the oxygen spectra. The intensity minimum³⁰⁾ in the O 1s XA profile of Fe_2O_3 at 532 eV results in an insignificant contribution to the XAS of $\text{PrFeAsO}_{1-\delta}$ at this energy. Thus, the small amount of unreacted Fe_2O_3 has a negligible effect on the oxygen XA spectra.

Figures 6(a) and (b) show the XAS and XES profiles of, Fe-metal, FeO and $\text{PrFeAsO}_{1-\delta}$. The ratio $I(L_2)/I(L_3)$ of the integrated intensities of the XES L_2 and L_3 peaks is given in Fig. 6(c). $\text{PrFeAsO}_{1-\delta}$ possesses an $I(L_2)/I(L_3)$ value that is identical to that of other FeAs materials such as CaFe_2As_2 ⁸⁾ and LiFeAs .²⁸⁾ Kurmaev *et al.*,²⁸⁾ in the case of other iron arsenides, noted the proximity of their $I(L_2)/I(L_3)$ values to that of Fe-metal. The $I(L_2)/I(L_3)$ value of $\text{PrFeAsO}_{1-\delta}$ suggests that the room-temperature character of $\text{PrFeAsO}_{1-\delta}$ is more metallic than insulating. The valence band (VB) of $\text{PrFeAsO}_{1-\delta}$ consists primarily of Fe 3d orbitals. Figure 6(d) shows VB spectral weight due to the Fe L_3 XE peak. The non-resonant profile possesses a single dominant peak and a low-energy shoulder in agreement with the findings of other x-ray studies.⁸⁾ The main peak is due primarily to Fe 3d bands^{8,32-33)} and we interpret the shoulder near 704 eV to originate from the hybridization of Fe 3d and As 4p states.⁷⁾ This assignment is supported by LDSA+*U* calculations which show that the spectral weight ~ 3.0 eV below E_F derives from both Fe and arsenic states.¹⁷⁾ An important question is whether Fe XES can be used to ascertain information about the bandwidth of the Fe 3d states. A measurement of the XES full-width at half maximum (FWHM) yields a width of 3.1 eV; however, this value is core-hole lifetime and multiplet broadened and cannot be taken as a direct measurement of the Fe 3d bandwidth. The width (~ 2 eV) of the dominant portion of the Fe L_3 XE peak can serve as a guide for the upper limit of the Fe 3d W . A range of reported values for the Coulomb parameter U , from 0.8 eV³⁴⁾ for a basis consisting of only Fe 3d orbitals to 2 eV^{18-19,35)} for a As *p* - Fe 3d mixing model,³⁵⁻³⁶⁾ is consistent with our O and iron spectra. Recently, Wang *et al.*⁹⁾ argued that $U \leq 2$ eV based on theoretical calculations that matched x-ray spectroscopy in the limiting condition. These values imply that the magnitude

of U is similar to or less than that of the estimated Fe $3d$ bandwidth. Importantly, the relative magnitude of U and W can implicate the extent of electron correlations in $\text{PrFeAsO}_{1-\delta}$. $U/W \sim 1$ implies weak to intermediate correlations due to the competition between the localizing effect of U and the itinerancy inherent in W ; $U/W > 1$ indicates strong electronic correlation.³⁷⁾ In the present case, $U/W \sim 1$ suggests that $\text{PrFeAsO}_{1-\delta}$ system is in an intermediate state between the metallic and insulating phases.^{7,18)}

In Fig. 7(a) we present a magnified view of the low-energy tail of the Fe L_3 XAS peaks of $\text{PrFeAsO}_{1-\delta}$ ($\delta = 0.15, 0.30$ and 0.35). The peak onset (see the arrow), defined as 10 percent of the absorption peak maximum, shifts subtly as a function of doping. The onset's upward shift of ≈ 900 meV to higher energies is due to the addition of electrons at Fe metallic sites. Equivalently, the onset shifts represent a reduction in the XAS intensity (hole DOS) near the Fermi-level. Figure 7(b) shows normalized XAS profiles juxtaposed to the Fe L -edge XES. XES reveals no significant differences among the various samples of the doped compounds. It is instructive to combine the Fe L -edge XAS and XES of $\text{PrFeAsO}_{1-\delta}$ in order to compare the composite intensity profiles of all the doped $\text{PrFeAsO}_{1-\delta}$ samples. If $\text{PrFeAsO}_{1-\delta}$ is taken to be metallic, the Fermi-level E_F can be approximated as the intersection of the Fe XE and XA spectral profiles. Fe $2p$ XA and Fe L -edge XE spectral intersection points are reduced relative to the valence and conduction band maxima. In addition, these points shift (Fig. 7(b)) by ≈ 200 meV on account of the doping δ . A closer examination of this shift is afforded by the left inset of Fig. 7(b) where the arrows indicate the positions of the points of intersection of the XA and XE spectra. The Fe L_3 XAS main-line shifts by ~ 0.15 eV upward with doping from $\delta = 0.15$ to 0.35 ; therefore, the Fe conduction band (CB) maximum and low-energy electronic structure *i.e.*, the onset, undergoes an observable change as a result of doping. The change in the onset of Fe XA L_3 peak over the doping range ($\delta = 0.15$ to 0.35) reflects the addition of doped electrons to the low-energy Fe states. The removal of low energy (near- E_F) unoccupied spectral weight is equivalent to electron addition per Fe atom. Reductions in the hole states

near the Fermi-level are accompanied by a systematic increase in the hole DOS at the Fe-As hybridization peak (shoulder). These changes in the high energy shoulder of the Fe L_3 -edge XA peak suggest that, concomitant with the addition of electrons to states near E_F , doping induces the removal of electrons from covalent bonding states associated with Fe and As atoms. The DOS at the Fermi-level $D(E_F)$, (right inset of Fig. 7(b)) increases as the doping decreases in agreement with the prediction of Singh and Du, giving a signal of a possible approach toward a parent phase magnetic instability³⁸⁻³⁹⁾ which experimental results show must be to an antiferromagnetic state. The trend also suggests that the parent compound is in the itinerant magnetism regime. It has not yet been determined whether the driving mechanism of the magnetic instability in iron-arsenide parent compounds is due to strong coupling or electron itinerancy. While the spin-density wave (SDW) in LaFeAsO was suggested to originate from the Fermi-surface nesting⁴⁰⁾ of electron and hole pockets an alternative proposal argued that the super exchange interaction of Fe ions mediated through the off-plane As atom was important.^{32,41-42)} The doping behavior of the Fe L_3 XAS shoulder is consistent with the notion that the Fe-As bonding might play an important role in the occurrence of the magnetic instability of the parent phase. Therefore, XES offers a method to access the link between the electronic structure at the Fermi-level and the magnetic behavior in FeAs superconductors.

4. Conclusion

In conclusion, by probing the oxygen and iron soft x-ray edges we have determined the behavior and structure of the low-lying electronic states of $\text{PrFeAsO}_{1-\delta}$ as a function of doping. The oxygen XAS and XES are well-described by LDA + small- U , LSDA and, DMFT calculations; however, only LDA + small- U matches the observed low energy O DOS just above and below E_F . The results indicate that the oxygen density of states of $\text{PrFeAsO}_{1-\delta}$ is well hybridized and is consistent with a band structure models for this material. The O $2p$

states are shown to be involved in long-range mixing, into the FeAs hybridized states, which might facilitate electron transfer between the layers. This mechanism, which is long-range and non-planar, is consistent with the report of three-dimensional superconductivity and the magnetism in some FeAs materials. We observe PrFeAsO_{1- δ} occupied and unoccupied O bands to have spectral features, throughout a full of oxygen vacancy doping range, that are similar to those observed in fluorine-doped materials *RE*-FeAsO_{1- x} F_{*x*}. Doping dependent energy shifts in the onset of the Fe unoccupied band, as given by Fe XAS, are consistent with electron doping despite the presence of extraneous spectral weight in the Fe XAS signal. The Fermi-level density of states $D(E_F)$ is observed to increase as the parent phase is approached; a signature of the tendency toward itinerant magnetism with decreasing doping. The detailed extent to which band structural models apply, as well as the nature of the mechanism of superconductivity will require continued investigation. With this in mind, the spectral labeling presented here is based on the best theoretical interpretations to-date. We believe that the experimental spectra given here are robust and should guide future theoretical models and understanding.

Acknowledgment

The authors would like to acknowledge important communications with G. Sawatzky and I. S. Elfimov. This work was supported by the U.S. Department of Energy, under Contract No. DE-AC02-05CH11231 and Office of Basic Energy Sciences U.S. DOE under Contract No. DE-AC03-76SF008. P.M.S. is grateful to the Japan Society for the Promotion of Science for the JSPS postdoctoral fellowship.

- 1) Y. Kamihara, T. Watanabe, M. Hirano, and H. Hosono: *J. Am. Chem. Soc.* **130** (2008) 3296.
- 2) Ren Zhi-An, Lu Wei, Yang Jie, Yi Wei, Shen Xiao-Li, Zheng-Cai, Che Guang-Can, Dong Xiao-Li, Sun Li-Ling, Zhou Fang and Zhao Zhong-Xian: *Chinese Physics Letters* **25** (2008) 2215; Zhi-An Ren, Guang-Can Che, Xiao-Li Dong, Jie Yang, Wei Lu, Wei Yi, Xiao-Li Shen, Zheng-Cai Li, Li-Ling Sun, Fang Zhou and Zhong-Xian Zhao: *Europhys. Lett.* **83** (2008) 17002.
- 3) Marianne Rotter, Marcus Tegel, Dirk Johrendt, Inga Schellenberg, Wilfried Hermes, and Rainer Pöttgen: *Phys. Rev. B* **78** (2008) 020503.
- 4) F. Ma and Z.-Y. Lu: *Phys. Rev. B* **78** (2008) 033111.
- 5) Gianluca Giovannetti, Sanjeev Kumar and Jeroen van den Brink: *Physica B* **403** (2008) 3653.
- 6) I. I. Mazin, I. Mazin, M. D. Johannes, L. Boeri, K. Koepernik, and D. J. Singh: *Phys. Rev. B* **78** (2008) 0851104.
- 7) Haule, J. H. Shim, and G. Kotliar: *Phys. Rev. Lett.* **100** (2008) 226402.
- 8) E. Z. Kurmaev, J. A. McLeod, A. Buling, N. A. Skorikov, A. Moewes, M. Neumann, M. A. Korotin, Yu. A. Izyumov, N. Ni, and P. C. Canfield: *Phys. Rev. B* **80** (2009) 054508.
- 9) W. L. Yang, A. P. Sorini, C.-C. Chen, B. Moritz, W.-S. Lee, F. Vernay, P. Olalde-Velasco, J. D. Denlinger, B. Delley, J.-H. Chu, J. G. Analytis, I. R. Fisher, J. Yang, W. Lu, Z. X. Zhao, J. van den Brink, Z. Hussain, Z.-X. Shen, and T. P. Devereaux: *Phys. Rev. B* **80** (2009) 014508.
- 10) D. H. Lu, M. Yi, S.-K. Mo, A. S. Erickson, J. Analytis, J.-H. Chu, D. J. Singh, Z. Hussain, T. H. Geballe, I. R. Fisher & Z.-X. Shen: *Nature* **455** (2008) 81.
- 11) D.R. Garcia, C. Jozwiak, C.G. Hwang, A. Fedorov, S.M. Hanrahan, S.D. Wilson, C.R. Rotundu, B.K. Freelon, R.J. Birgeneau, E. Bourret-Courchesne and A. Lanzara: *Phys. Rev. B* **78** (2008) 245119.
- 12) C. Cao, P. J. Hirschfeld, and H.-P. Cheng: *Phys. Rev. B* **77** (2008) 220506.
- 13) K. Miyazawa, K. Kihou, P. M. Shirage, C. H. Lee, H. Kito, H. Eisaki, and A. Iyo, J.: *Phys. Soc. Jpn.* **78** (2008) in press.
- 14) K. Hashimoto, T. Shibauchi, T. Kato, K. Ikada, R. Okazaki, H. Shishido, M. Ishikado, H. Kito, A. Iyo, H. Eisaki, S. Shamoto, Y. Matsuda: *Phys. Rev. Lett.* **102** (2009) 017002.
- 15) P. M. Shirage, K. Miyazawa, M. Ishikado, K. Kihou, C. H. Lee, N. Takeshita, H. Matsuhata, R. Kumai, Y. Tomioka, T. Ito, H. Kito, H. Eisaki, S. Shamoto and A. Iyo: *Physica C* **469** (2009) 355.

- 16) C.H. Lee, A. Iyo, H. Eisaki, H. Kito, M.T. Fernandez-Diaz, T. Ito, K. Kihou, H. Matsuhata, M. Braden, and K. Yamada: J. Phys. Soc. Jpn. **77** (2008) 083704.
- 17) D. J. Singh and M.-H. Du: Phys. Rev. Lett. **100** (2008) 237003.
- 18) G. A. Sawatzky, I. S. Elfimov, J. van den Brink, and J. Zaanen: Europhys. Lett. **86** (2009) 17006.
- 19) I. A. Nekrasov, Z. V. Pchelkina, and M. V. Sadovskii: JETP Lett. **87** (2008) 560.
- 20) F. Ma and Z.-Y. Lu: Phys. Rev. B **78** (2008) 033111.
- 21) T. Kroll, S. Bonhommeau, T. Kachel, H.A. Dürr, J. Werner, G. Behr, A. Koitzsch, R. Huebel, S. Leger, R. Schoenfelder, A. Ariffin, R. Manzke, F.M.F. de Groot, J. Fink, H. Eschrig, B. Buechner, M. Knupfer: Phys. Rev. B **78** (2008) 220502.
- 22) D. J. Singh: private communication (2009).
- 23) F. Bondino, E. Magnano, M. Malvestuto, F. Parmigiani, M. A. McGuire, A. S. Sefat, B. C. Sales, R. Jin, D. Mandrus, E.W. Plummer, D. J. Singh, and N. Mannella: Phys. Rev. Lett **101** (2008) 267001.
- 24) R. D. Leapman and L. A. Grunes: Phys. Rev. Lett. **45** (1980) 397.
- 25) B. T. Thole and G. van der Laan: Phys. Rev. B **38** (1988) 3158.
- 26) Frank M. F. de Groot, Pieter Glatzel, Uwe Bergmann, Peter A. van Aken, Raul A. Barrea, Stephan Klemme, Michael Hävecker, Axel Knop-Gericke, Willem M. Heijboer, and Bert M. Weckhuysen: J. Phys. Chem. B **109** (2005) 20751.
- 27) D. Nolle, E. Goering, T. Tietze, G. Schütz, A. Figuerola and L. Manna: New. J. Phys. **11** (2009) 033034.
- 28) E. Z. Kurmaev, J. A. McLeod, N. A. Skorikov, L. D. Finkelstein, A. Moewes, Yu A Izyumov and S. Clarke: J. Phys. Condens. Matter **21** (2009) 345701.
- 29) F. M. F. de Groot, M. Grioni, J. C. Fuggle, J. Ghijsen, G. A. Sawatzky and H. Petersen: Phys. Rev. B **40** (1989) 5715.
- 30) J. A. Liero, G. Drager and W. Czolbe: X-ray Spectroscopy **22** (1993) 272.
- 31) A recent report by Nie et. al., arXiv:0912.4539v1, suggests that oxidation of Fe-based samples or starting materials might contribute to changes in the *intensity* of the O 1s XAS pre-peak if the exposure to O₂ sufficient. The lack of dual iron-oxide pre-peaks and the absence of change in the pre-peak intensity of the PrFeAsO samples supports our claim that the unreacted Fe₂O₃ has a negligible effect on the oxygen XA spectra.
- 32) K. Schwarz, A. Neckel and J. Nordgren: J. Phys. F: Metal Phys. **9** (1979) 2509.
- 33) G. van der Laan and I. W. Kirkman: J. Phys. Condens. Matter **4** (1992) 4189.

- 34) V. I. Anisimov, Dm. M. Korotin, A. V. Kozhevnikov, J. Kunes, A. O. Shorikov, S. L. Skornyakov and S. V. Streltsov: *J. Phys. Condens. Matter* **21** (2009) 075602.
- 35) Jiansheng Wu, Philip Phillips, and H. Castro Neto: *Phys. Rev. Lett.* **101** (2008) 126401.
- 36) V. Cvetkovic and Z. Tesanovic: *Europhys. Lett.* **85** (2009) 37002.
- 37) G. A. Sawatzky, J. Zaanen and J. W. Allen: *Phys. Rev. Lett.* **55** (1985) 418.
- 38) R. Skomski: *Simple Models of Magnetism* (Oxford University Press, Oxford, 2008) pg. 121.
- 39) I. I. Mazin, D. J. Singh, M. D. Johannes and M.H. Du: *Phys. Rev. Lett.* **101** (2008) 057003.
- 40) J. Dong, H. J. Zhang, G. Xu, Z. Li, G. Li, W. Z. Hu, D. Wu, G. F. Chen, X. Dai, J. L. Luo, Z. Fang and N. L. Wang: *Europhys. Lett.* **83** (2008) 27006.
- 41) T. Yildirim: *Phys. Rev. Lett.* **101** (2008) 057010.
- 42) Q. Si and E. Abrahams: *Phys. Rev. Lett.* **101** (2008) 076401.

Figure Captions Freelon *et. al.*,

Fig. 1. (color online) The crystal structure of $\text{PrFeAsO}_{1-\delta}$ in the high temperature $P4/nmm$ tetragonal phase.

Fig. 2. (a) Oxygen $1s$ x-ray absorption spectra of $\text{PrFeAsO}_{1-\delta}$ ($\delta = 0.15, 0.30$ and 0.35) taken in total fluorescence yield (TFY) mode. Feature **A** is the oxygen pre-peak due to O-Fe $3d$ and As $4p$ hybridization; **B** is an O-Pr $5d$ hybridization peak. Features **A**, **B** and **C** (see inset) do not shift with respect to oxygen vacancy concentration.

Fig. 3. Normalized O $1s$ XA and O $K\alpha$ XE spectra of $\text{PrFeAsO}_{1-\delta}$ ($\delta = 0.15, 0.30$ and 0.35). The XES(XAS) reflect the occupied(unoccupied) oxygen partial density of states. The major spectral features I-IV, **A**, **B** and **C** are discussed in the text.

Fig. 4. Fe L -edge X-ray absorption and emission spectra of $\text{PrFeAsO}_{0.85}$ $T_c = 3$ K. (a) the total electron yield (TEY) mode Fe $2p$ XA intensity plotted as a function of photon energy. (b) The non-resonant Fe L -edge XE intensity profile collected at an incident energy of 740 eV.

Fig. 5. The Fe TFY L_3 XAS band of (a) raw $\text{PrFeAsO}_{1-\delta}$ ($\delta = 0.15, 0.30$ and 0.35). Both raw $\text{PrFeAsO}_{0.70}$ (b) and Fe_2O_3 (c) Fe L_3 XA spectra are shown with fitted curves (gray lines) based on Gaussian functions (see text). (d) $\text{PrFeAsO}_{0.70}$ Fe L_3 XA spectrum.

Fig. 6. A Comparison of Fe $2p$ XAS and Fe $L_{2,3}$ XES data of FeO, $\text{PrFeAsO}_{0.85}$ and Fe-metal. (a) X-ray absorption spectra and (b) x-ray emission spectra. (c) The $\text{PrFeAsO}_{0.85}$ Fe L_3 XES peak (dotted circle) is fitted (solid) with two Gaussian peaks. (d) The ratio $I(L_2)/I(L_3)$ of the integrated XES main peak intensities of samples FeO, Fe-metal and $\text{PrFeAsO}_{0.85}$.

Fig. 7. Enhanced views of the normalized Fe $2p$ XA and Fe $L_{2,3}$ XE spectra of $\text{PrFeAsO}_{1-\delta}$ ($\delta = 0.15, 0.30$ and 0.35). (a) The onset of the leading edge of the Fe L_3 XA edge undergoes a shift as a function of oxygen vacancy doping. (b) The XE and XA spectra are juxtaposed in order to depict the Fe band occupied and unoccupied electronic bandstructure versus doping. XE spectra, collected at an incident photon energy of 740 eV, do not change with doping. Fe $2p$ XA spectra show that the conduction band maximum does not shift with electron doping. A shift in the chemical potential is revealed (inset) as a change in the normalized intensity of the XE and XA spectral intersection.

Figure 1, Freelon *et. al.*,

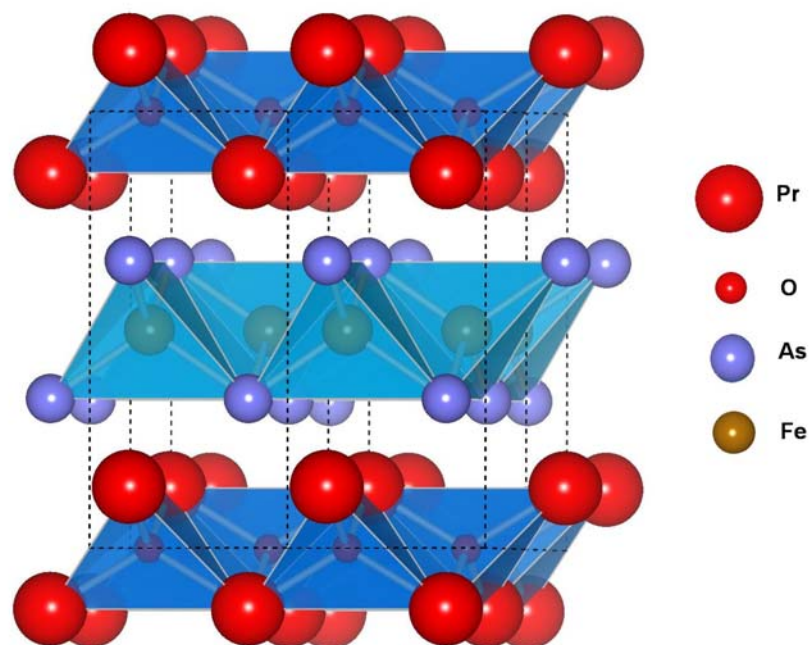


Fig. 1. (color online) Crystal structure of $\text{PrFeAsO}_{1.8}$ in the high temperature $P4/nmm$ tetragonal phase.

Figure 2, Freelon *et. al.*,

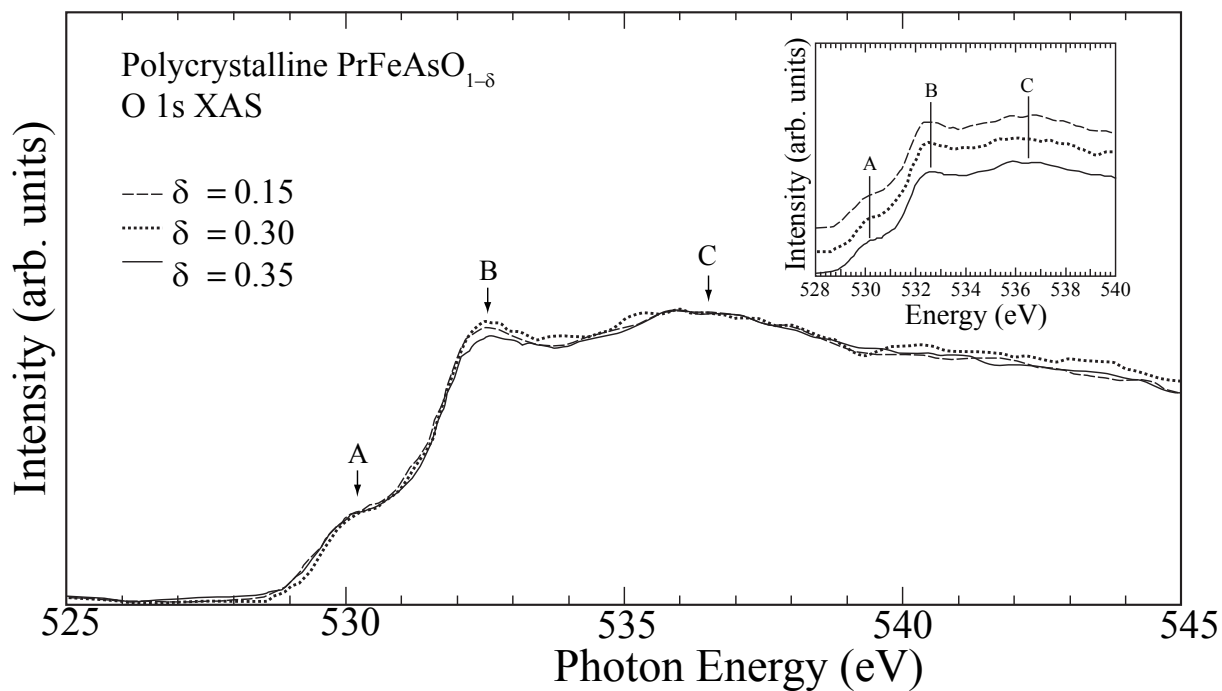


Fig. 2. (a) Oxygen 1s x-ray absorption spectra of $\text{PrFeAsO}_{1-\delta}$ ($\delta = 0.15, 0.30$ and 0.35) taken in total fluorescence yield (TFY) mode. Feature A is the oxygen pre-peak due to O-Fe 3d and As 4p hybridization; B is an O-Pr 5d hybridization peak. Features A, B and C (see inset) do not shift with respect to oxygen vacancy concentration.

Figure 3, Freelon *et. al.*,

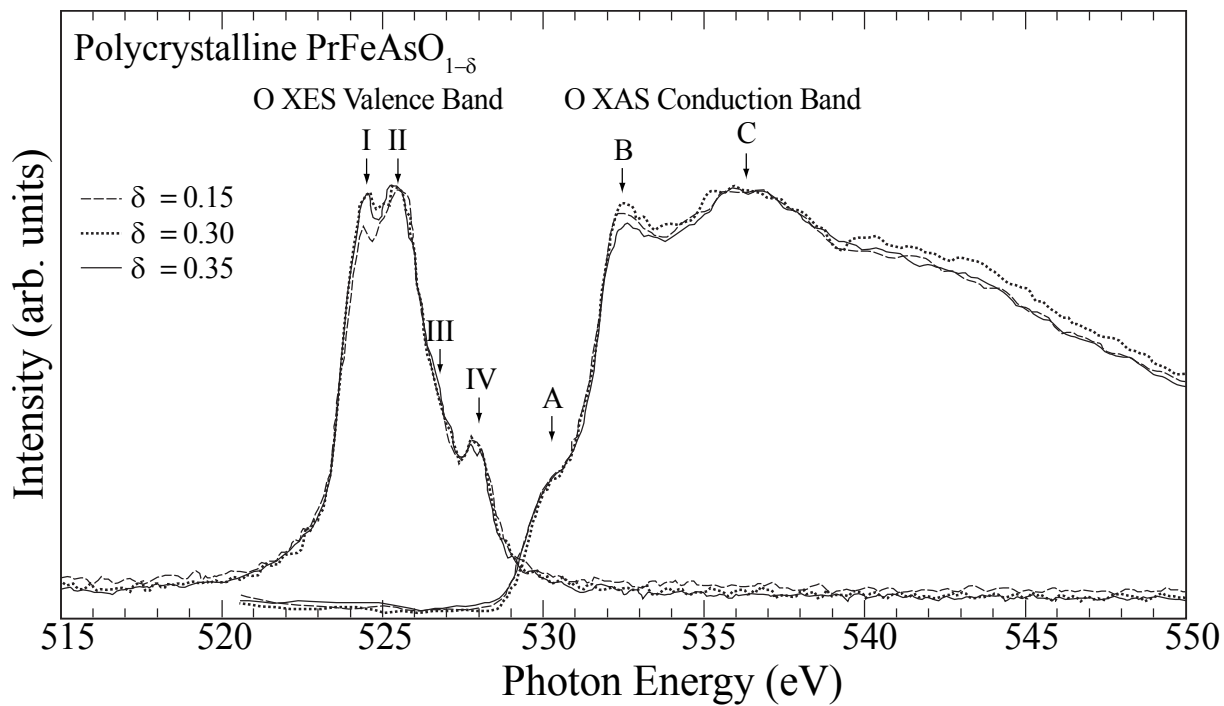


Fig. 3. Normalized O $1s$ XA and O $K\alpha$ XE spectra of PrFeAsO_{1-δ} ($\delta = 0.15, 0.30$ and 0.35). The XES(XAS) reflect the occupied(unoccupied) oxygen partial density of states. The major spectral features **I-IV**, **A**, **B** and **C** are discussed in the text.

Figure 4, Freelon *et al.*,

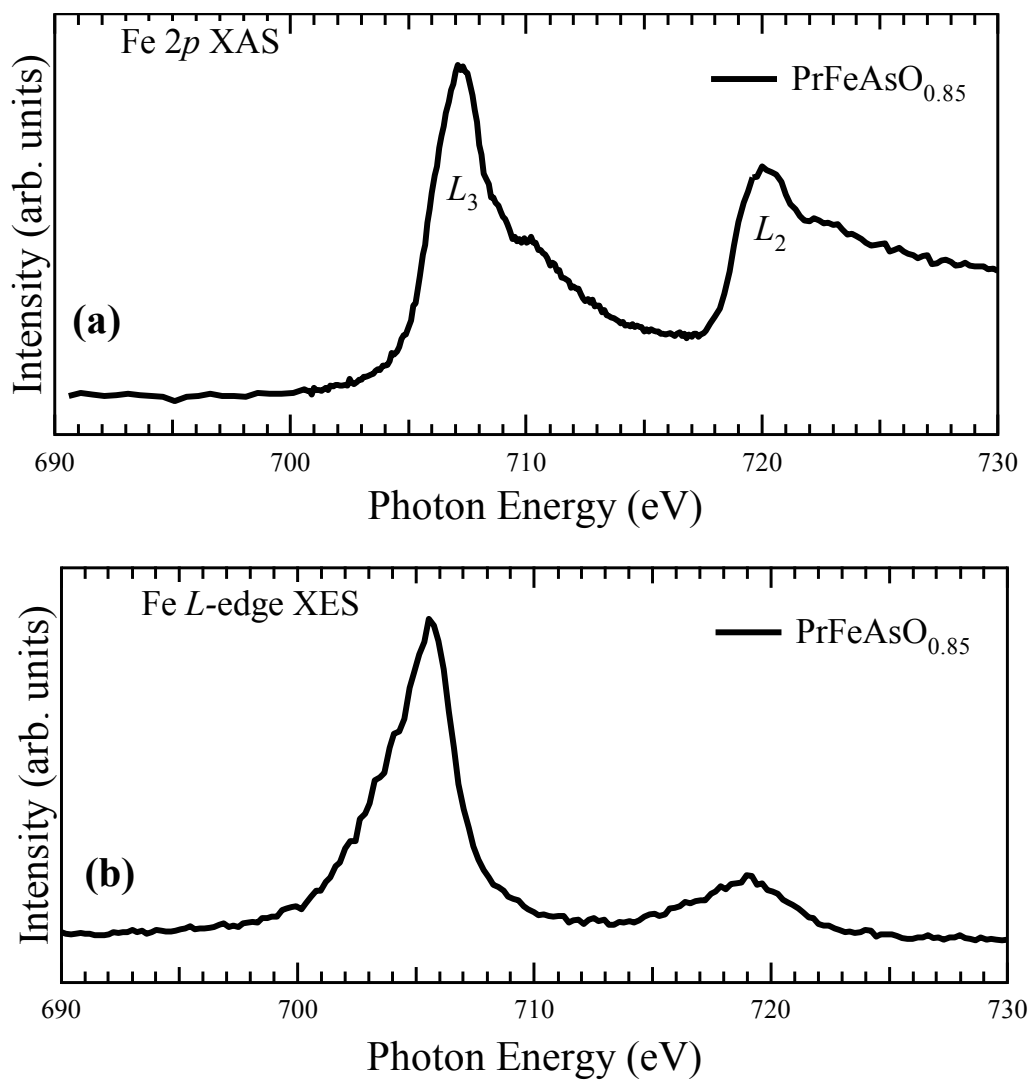


Fig. 4. Fe *L*-edge X-ray absorption and emission spectrum of PrFeAsO_{0.85} T_c = 3 K. (a) the total fluorescence yield (TFY) mode Fe 2*p* XA intensity plotted as a function of photon energy. (b) The non-resonant Fe *L*-edge XE intensity profile collected at an incident energy of 740 eV.

Figure 5, Freelon *et al.*,

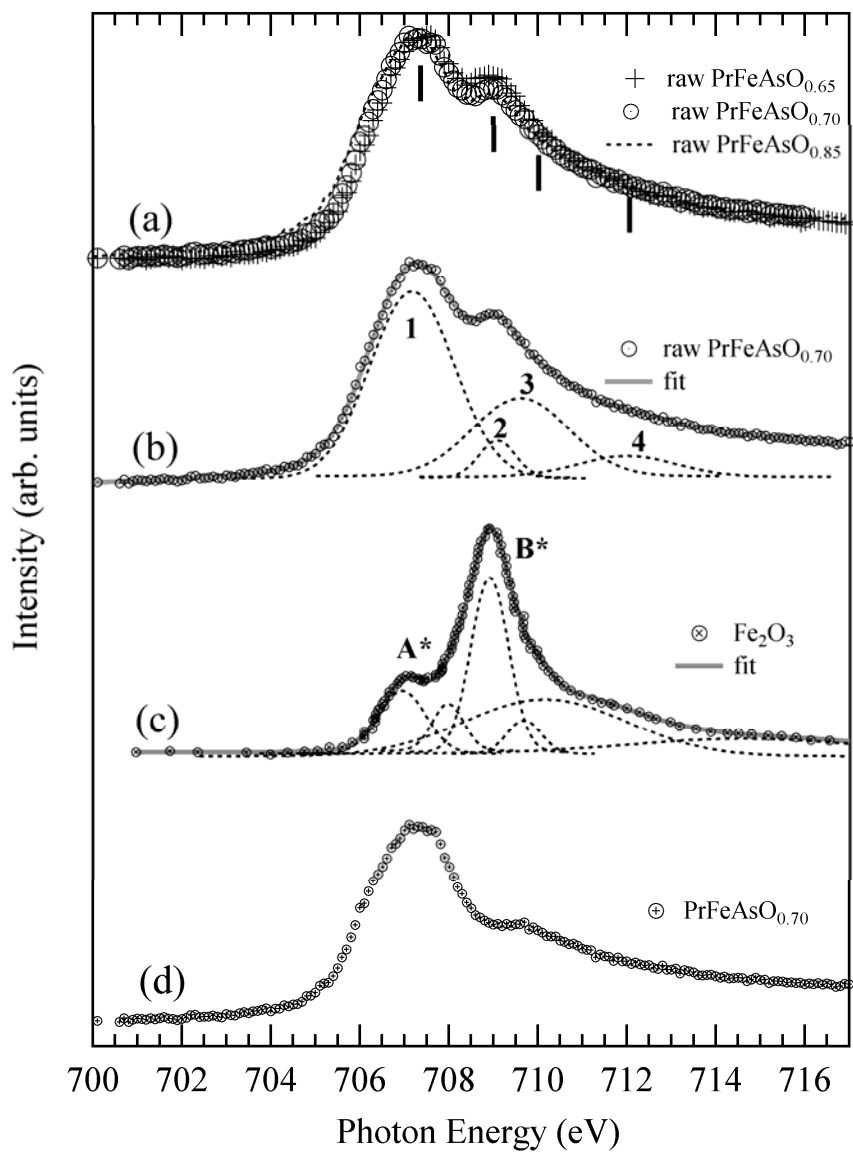


Fig. 5. The Fe TFY L_3 XAS band of (a) raw PrFeAsO $_{1-\delta}$ ($\delta = 0.15, 0.30$ and 0.35). Both raw PrFeAsO $_{0.70}$ (b) and Fe $_2$ O $_3$ (c) Fe L_3 XA spectra are shown with fitted curves (gray lines) based on Gaussian functions (see text). (d) PrFeAsO $_{0.70}$ Fe L_3 XA spectrum.

Figure 6, Freelon *et al.*,

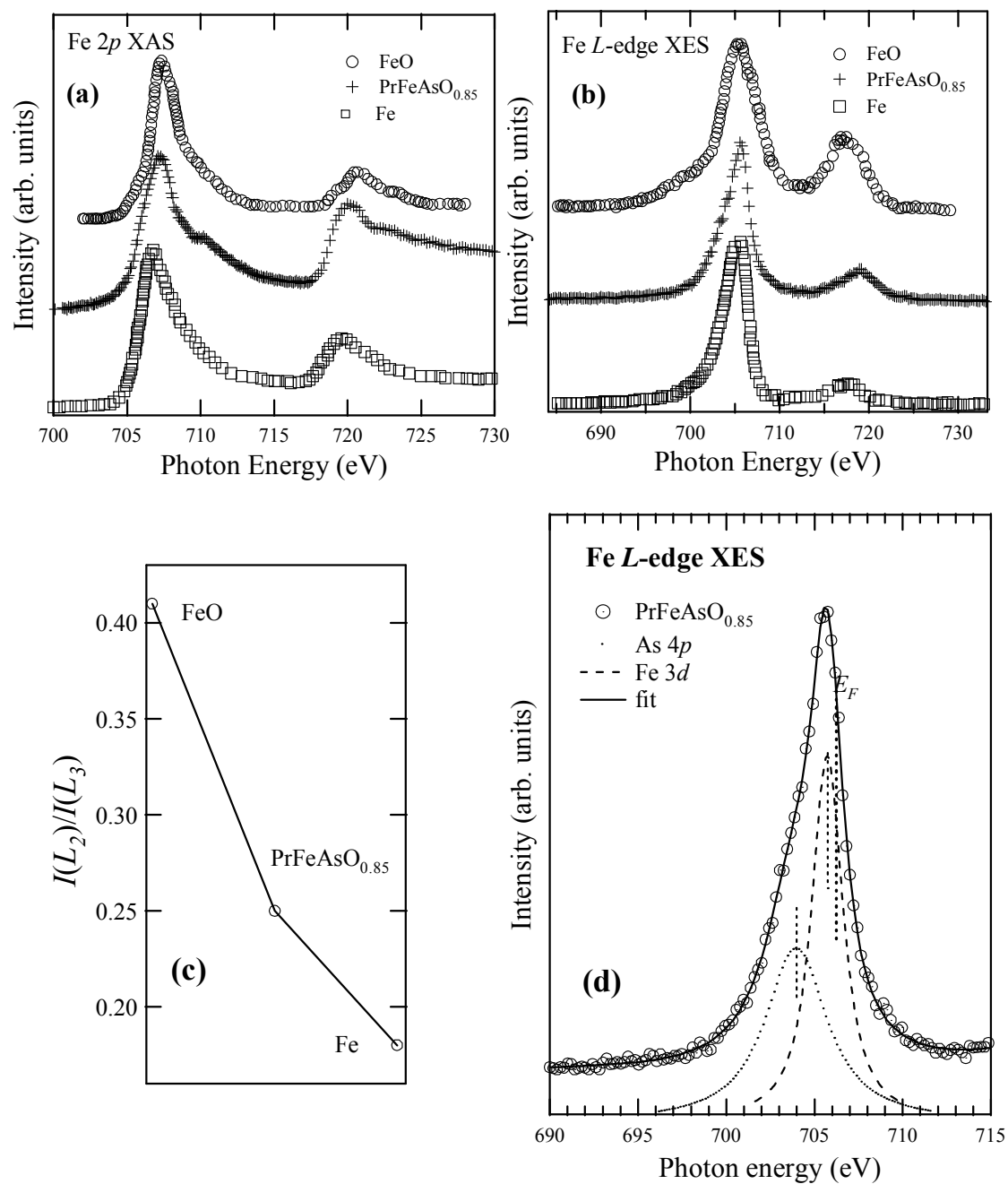


Fig. 6. A Comparison of Fe 2p XAS and Fe L_{2,3} XES data of FeO, PrFeAsO_{0.85} and Fe-metal. (a) X-ray absorption spectra and (b) x-ray emission spectra. (c) The ratio $I(L_2)/I(L_3)$ of the integrated XES main peak intensities of samples FeO, Fe-metal and PrFeAsO_{0.85}. (d) The PrFeAsO_{0.85}Fe L₃ XES peak (dotted circle) is fitted (solid) with two Gaussian peaks.

Figure 7, Freelon *et al.*,

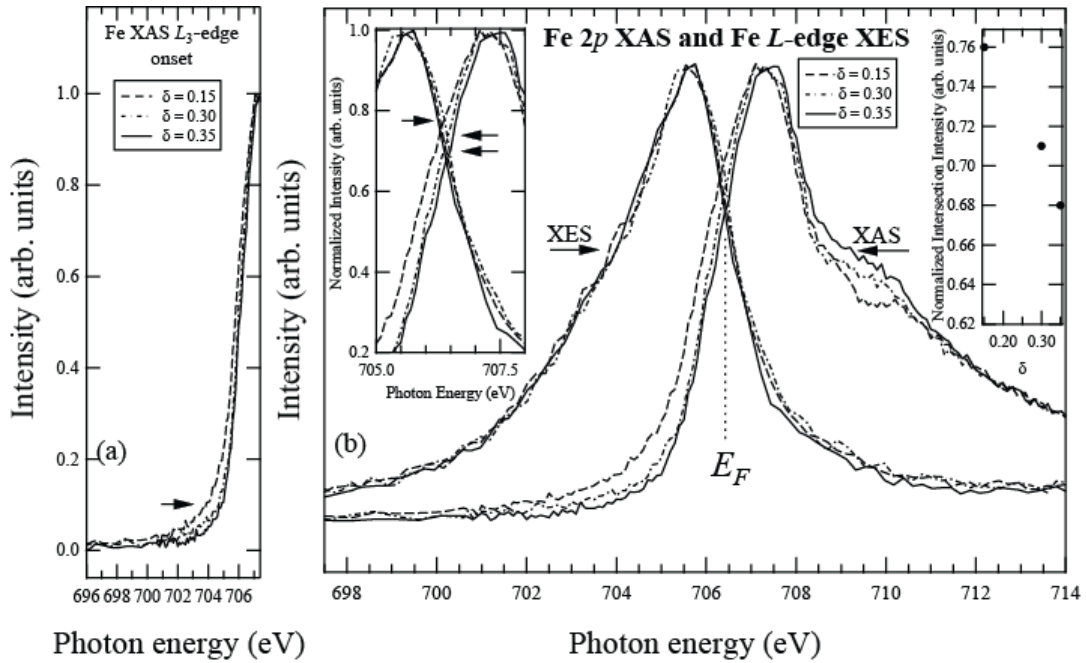


Fig. 7. Enhanced views of the normalized Fe 2p XA and Fe $L_{2,3}$ XE spectra of PrFeAsO_{1- δ} ($\delta = 0.15, 0.30$ and 0.35). (a) The leading edge of the Fe L_3 XA edge undergoes a subtle shift as a function of oxygen vacancy doping. (b) The XE and XA spectra are juxtaposed in order to depict the Fe band occupied and unoccupied electronic structure versus doping. The XE spectra, collected at an incident photon energy of 740 eV, do not change with doping. Fe 2p XA spectra show that the conduction band maximum does not shift with electron doping. A shift in the chemical potential is revealed (inset) as a change in the normalized intensity of the XE and XA spectral intersections.